Journal of Materials and Electronic Devices 2 (2025) 14-19

JOURNAL OF MATERIALS AND ELECTRONIC DEVICES
JMED

Enhanced Photoelectrical Performance of Al/p-Si/ZnO:B_4C/Al Photodiodes Fabricated via the Sol-Gel Spin-Coating Technique

[1]Mahmud ALLAVI,[1*]Turan GURGENC

[1]Firat University, Technology Faculty, Automotive Engineering Department, Elazig, Turkey

In this study, Al/p-Si/ZnO:B_4C/Al structured photodiodes were fabricated using the sol-gel spin-coating method, and the effect of B_4C doping (0, 1, 3, 5, and 10 wt.%) on device performance was investigated. The thin films were characterized by FE-SEM and EDX analyses, confirming the formation of crack-free, homogeneous, and nanostructured surfaces on p-Si substrates. Electrical and photoresponse measurements were carried out under illumination intensities ranging from 20 to 100 mW cm^{-2}. At 100 mW cm^{-2}, the photocurrent values were determined as 56×10^{-4}, 16.4×10^{-5}, 6.97×10^{-5}, 3.43×10^{-5}, and 2.67×10^{-5} A for 0%, 1%, 3%, 5%, and 10% B_4C contents, respectively. It was observed that the photocurrent decreased with increasing B_4C concentration, although the photoresponse could be tuned by adjusting the doping level. The results demonstrate that ZnO:B_4C photodiodes were successfully fabricated and that their optoelectronic performance can be effectively controlled through the B_4C doping ratio.

Keywords: *ZnO, Boron carbide, Photodiode, Sol-gel spin coating.*

Submission Date: 24 July 2025
Acceptance Date: 11 November 2025

**Corresponding author: tgurgenc@firat.edu.tr*

1. Introduction

Photodiodes are semiconductor devices that convert light into electrical signals and are widely used in solar energy conversion and optoelectronic detection systems due to their fast response and low power consumption. The efficiency of these devices is directly influenced by the bandgap of the material used, the quality of the interface, and the fabrication technique. Schottky, p-n, p-i-n, and heterojunction structures each exhibit distinct carrier transport dynamics and reverse leakage characteristics. In recent years, in metal oxide–based photodiodes, strategies such as doping and composite formation have gained importance for reducing interface traps and controlling band alignment. In this context, the incorporation of nanoparticles into semiconductor matrices has been shown to modify carrier concentration, surface roughness, and energy barriers, thereby directly influencing photocurrent generation and light sensitivity. The interfacial interactions induced by nanoparticle addition can enhance the response speed and stability of photodiodes under illumination.

Furthermore, studies on semiconductor metal oxide–based systems have demonstrated that the doping concentration can significantly improve key parameters such as photocurrent and responsivity, and that both solution-processed and vacuum-deposited structures can exhibit tunable I-V and I-t characteristics depending on light intensity [1-5].

ZnO, with its wide direct bandgap (approximately 3.2-3.4 eV), high exciton binding energy, optical transparency in the visible region, and n-type conductivity, is one of the most widely used oxide semiconductors in optoelectronic applications such as photodiodes, ultraviolet detectors, and solar cells. Its ability to be fabricated at relatively low temperatures, together with its chemical stability and ease of doping, makes ZnO an advantageous material for composite

structure development. The incorporation of nanoparticles into the ZnO matrix can alter the work function and depletion region width, thereby influencing charge carrier separation and recombination mechanisms, which directly determine the magnitude of the photoelectric response. Boron carbide (B_4C) is an advanced ceramic material known for its high hardness, chemical stability, low density, and structural integrity even at elevated temperatures. With a high melting point (around 2450 °C), a wide bandgap, and low electrical conductivity, B_4C is regarded as a thermally and electrically stable material. Owing to its stable electronic configuration, when combined with semiconductor matrices, B_4C can modify carrier transport pathways and interface potential barriers, enabling better control over the electrical parameters of the device. When integrated with ZnO, B_4C interacts with the n-type conductivity of ZnO, forming new energy levels at the interface and reducing the probability of carrier recombination. Consequently, this combination can suppress dark current and improve current stability under forward bias, leading to enhanced and more reliable photodiode performance [5-9].

The choice of fabrication method plays a crucial role in determining the overall performance of a photodiode, as it directly affects the interface integrity and film thickness. Among the various thin-film deposition techniques based on the sol-gel process, the spin-coating method stands out due to its low cost, non-vacuum operation, ability to produce uniform coatings over large areas, and ease of controlling film thickness and composition. In this method, a precursor solution is prepared and subjected to hydrolysis and gelation, after which it is deposited onto the substrate at a specific rotation speed. The process can be repeated to form multilayer structures if needed. A subsequent thermal annealing step improves crystallinity and removes residual organic components within the film. This controlled and reproducible fabrication route enables the production of high-quality, stable, and efficient photodiode structures, particularly in devices where interface quality critically influences optoelectronic performance [3, 10-12].

The main objective of this study is to investigate the potential of B_4C-doped ZnO composite structures in photodiode applications and to evaluate the influence of different doping concentrations on device performance. ZnO-based photodiodes have long been a focus of optoelectronic research due to their wide bandgap, high optical transparency, and chemical stability. However, the limited carrier separation efficiency and recombination losses at the interfaces in pure ZnO structures have highlighted the need for doping strategies to enhance device performance. In this context, the effects of B_4C incorporation on the electrical and optical properties of ZnO were examined, with particular attention to its impact on photocurrent generation, sensitivity, and operational stability of the photodiodes. Given its high chemical stability, low electrical conductivity, and distinct energy band structure, B_4C is expected to introduce new energy levels at the ZnO interface, thereby improving key parameters that determine photodiode performance. A detailed review of the literature revealed that while B_4C-doped ZnO structures have been investigated in sensor and photocatalytic applications, no prior studies have reported their use in photodiode fabrication. Therefore, the originality of this research lies in the first systematic evaluation of the effects of B_4C incorporation into ZnO-based photodiodes, aiming to enhance their optoelectronic performance and stability.

In this study, Al/p-Si/ZnO:B_4C/Al structured photodiodes were fabricated using the sol-gel spin-coating technique. Thin films with different B_4C doping ratios (0, 1, 3, 5, and 10 wt.%) were prepared, and their structural, morphological, electrical, and optoelectronic properties were comprehensively investigated. The surface morphology and structural features of the fabricated photodiodes were characterized using field emission scanning electron microscopy (FE-SEM) and energy-dispersive X-ray (EDX) analyses. The electrical and photoresponse behaviors of the devices were evaluated through current–voltage (I-V) and current–time (I-t) measurements under various illumination intensities. In addition, the influence of B_4C concentration on the reverse current, photocurrent, photoresponse, and responsivity of the photodiodes was quantitatively analyzed to assess the effect of doping on overall device performance.

2. Experimental Details

In this study, Al/p-Si/ZnO:B_4C/Al structured photodiodes were fabricated using the sol-gel spin-coating technique, and their structural, morphological, electrical, and optoelectronic properties were comprehensively investigated. The fabrication process consisted of three main stages: preparation of the substrate, deposition of pure and B_4C-doped ZnO thin films, and formation of the photodiode structure. P-type silicon (p-Si) wafers were used as substrates and were chemically cleaned to remove organic contaminants and metallic impurities. Initially, the substrates were ultrasonically cleaned in acetone for 5 minutes, followed by rinsing in deionized water, ethanol, and distilled water. Subsequently, the samples were immersed in a 1:10 hydrofluoric acid (HF) solution for 30 seconds to remove surface oxides, then rinsed in deionized water for 5 minutes and dried. Finally, the substrates were annealed in a nitrogen atmosphere at 570 °C for 5 minutes to ensure complete oxide removal and to prepare a clean, smooth surface for film deposition. Pure ZnO thin films were prepared by the sol-gel method. Zinc acetate dihydrate [$Zn(CH_3COO)_2.2H_2O$] supplied by Sigma-Aldrich was dissolved in 15 mL of methoxyethanol to form a 0.3 M solution, which was stirred at 700 rpm and 60 °C for 60

minutes. Monoethanolamine ($NH_2CH_2CH_2OH$) was then added as a stabilizing agent at a volume of 0.245 mL. The resulting sol was aged for 24 hours to complete homogenization and hydrolysis. The prepared sol was deposited onto the p-Si substrate by spin coating at 1000 rpm for 30 seconds, repeated twice to obtain two layers. Each layer was preheated at 150 °C for 15 minutes to remove residual solvents, followed by annealing at 450 °C for 1 hour to achieve film crystallization. For B_4C-doped ZnO thin films, the same procedure was applied, with the addition of B_4C nanoparticles in different weight percentages (1%, 3%, 5%, and 10%) into the ZnO sol. The B_4C nanoparticles (Nanografi, 99.5% purity, 40-60 nm particle size) were dispersed in the sol and stirred magnetically at 60 °C for 30 minutes, followed by ultrasonication for 10 minutes to ensure uniform dispersion. The resulting ZnO:B_4C sols were spin-coated on p-Si substrates under identical conditions and annealed at 450 °C for 1 hour to enhance crystallinity. To form the photodiode structure, aluminum (Al) top contacts were deposited onto the ZnO and ZnO:B_4C thin films using a thermal evaporation system. A physical mask was used during the deposition to define contact regions, and high-purity (99.99%) Al was evaporated to form the electrodes. This process resulted in the successful fabrication of Al/p-Si/ZnO:B_4C/Al photodiodes. The structural and morphological properties of the thin films were characterized using a ZEISS GEMINI 500 field emission scanning electron microscope (FE-SEM) equipped with an energy-dispersive X-ray (EDX) detector. FE-SEM was used to analyze surface morphology, while EDX measurements identified the elemental composition and verified the uniform distribution of Zn, O, B, and C within the films. The electrical and optoelectronic properties of the photodiodes were examined using a KEITHLEY 4200 semiconductor characterization system and a FYTRONIX solar simulator. Measurements were performed in the dark and under illumination intensities ranging from 20 to 100 mW/cm^2, provided by the solar simulator. Current-voltage (I-V) measurements were used to evaluate rectification behavior, reverse current, and photocurrent variations, while current-time (I-t) measurements were conducted to analyze transient photoresponse characteristics under periodic light on/off conditions.

3. Results and Discussion

Figure 1 presents the FE-SEM images and EDX analysis results of pure ZnO and ZnO:B_4C thin films with different B_4C concentrations deposited on p-Si substrates. The images reveal that all films were uniformly formed on the p-Si surface, exhibiting smooth, crack-free, and homogeneous coatings. The films display a nanostructured morphology with evenly distributed particles, and no signs of peeling or aggregation were observed on the surfaces. The EDX analysis confirmed the presence of Zn, O, B, and C elements in the film composition. In the pure ZnO film, the oxygen and silicon contents were determined as 52.48% and 45.55%, respectively, while zinc was measured at 1.97%. This result indicates that the ZnO layer was successfully formed on the p-Si substrate and that Zn was effectively incorporated into the film structure. For the film containing 1% B_4C, the Zn and O ratios were 2.25% and 51.02%, respectively, with trace amounts of boron (0.02%) and carbon (6.23%) detected. In the 3% B_4C-doped film, the elemental composition was Zn 2.22%, O 50.94%, B 0.02%, and C 6.64%, confirming that B_4C was homogeneously integrated into the ZnO matrix. At 5% B_4C content, Zn was 2.12%, O 51.48%, and C 6.66%, while at 10% B_4C, these values were Zn 2.36%, O 50.30%, and C 7.85%. A gradual increase in carbon content and a slight decrease in oxygen content were observed with increasing B_4C concentration. These results demonstrate that ZnO:B_4C thin films were successfully fabricated on p-Si substrates using the sol-gel spin-coating technique. Furthermore, as the B_4C content increased, the grain size of the films decreased, surface compactness improved, and the nanostructured morphology became more pronounced. While the pure ZnO films exhibited relatively larger grains in some regions, the B_4C-doped films showed finer and more uniform grain distributions. Similar trends have also been reported in previous studies employing different dopant materials, where structural improvement, grain size reduction, and enhanced surface homogeneity were observed in ZnO-based thin films [13-15]. This finding indicates that the obtained results are consistent with the literature and that the incorporation of B_4C has a beneficial effect on improving the morphological integrity of the ZnO thin films.

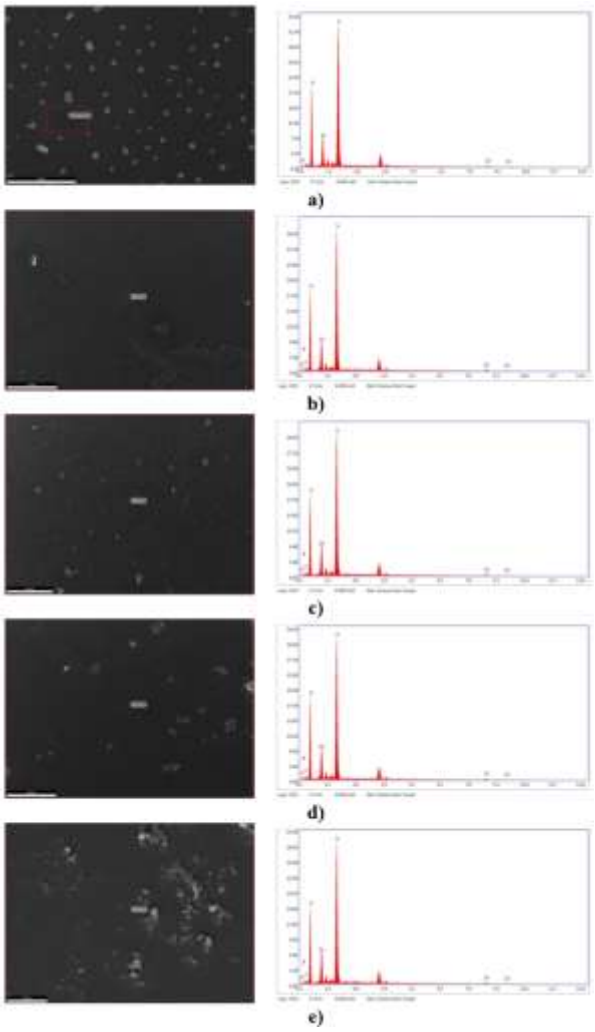

Figure 1. FE-SEM images and EDX graphs of a) ZnO, b) ZnO:1%B_4C, c) ZnO:3%B_4C, d) ZnO:5%B_4C and e) ZnO:10%B_4C devices.

Figure 2 presents the current-voltage (I-V) characteristics of the fabricated composite-based photodiodes measured in the dark and under varying illumination intensities ranging from 20 to 100 mW/cm^2. The results clearly indicate that variations in the B_4C content have a significant influence on the electrical performance of the photodiodes. Distinct differences between dark and illuminated conditions were observed, particularly in the reverse bias region. Under illumination, the reverse current values of the Al/p-Si/ZnO:B_4C/Al photodiodes were found to be higher than those measured in darkness at the same applied voltages. In the forward bias region, the current increased progressively with voltage, whereas deviations in the reverse current behavior reflected the rectifying nature of the diodes. As evident from the I-V curves, all photodiodes exhibit pronounced photoresponsivity. The variation of reverse current with bias can be attributed to the photon-induced excitation of charge carriers from the valence band to the conduction band. When light is incident on the photodiode surface, electron-hole pairs are generated, resulting in an increase in current with rising light intensity under reverse bias, while no substantial change is observed in the forward bias region. This behavior indicates that the generated free carriers effectively contribute to the photocurrent. The increase in reverse current with illumination confirms the photovoltaic nature of the fabricated Al/p-Si/ZnO:B_4C/Al photodiodes and demonstrates their sensitivity to light intensity [3, 16, 17].

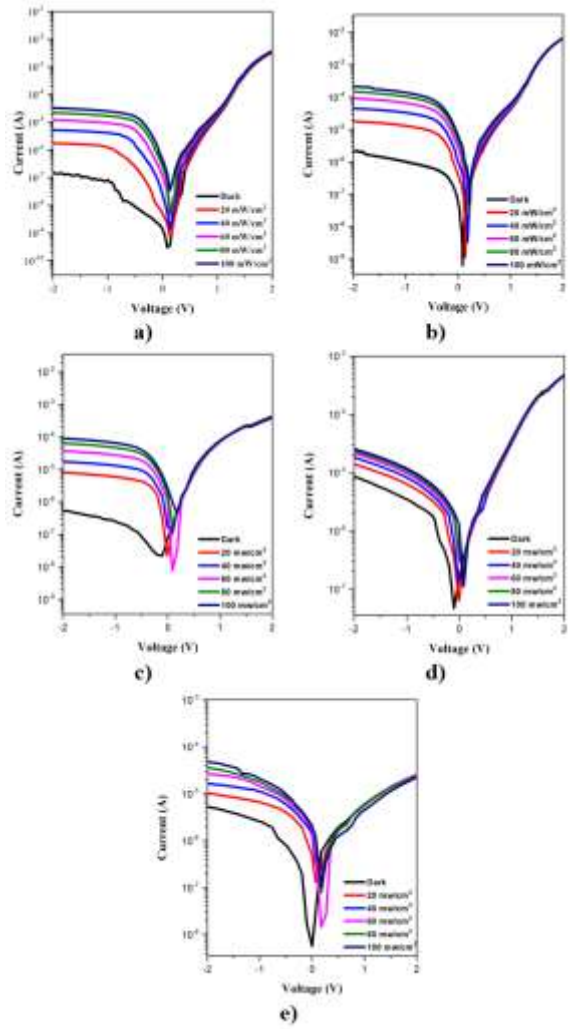

Figure 2. I-V graphs of a) ZnO, b) ZnO:1%B_4C, c) ZnO:3%B_4C, d) ZnO:5%B_4C and e) ZnO:10%B_4C devices.

Figure 3 shows the photosensitivity values of the photodiodes at -2 V, calculated according to the equation reported in the literature [3, 18]. All photodiodes exhibited higher reverse current values under illumination compared to dark conditions. The photodiode with the highest light sensitivity was found to be the undoped one. The photosensitivity of the devices increased with rising light intensity, and photodiodes with different sensitivities were obtained depending on the B_4C doping ratio. The incorporation of B_4C into ZnO altered the work function of ZnO, which consequently led to variations in the depletion

region width of the diode. This modification is believed to reduce charge separation under reverse bias, resulting in lower photosensitivity values for the nanocomposite photodiodes compared to pure ZnO. While high photosensitivity is desirable in certain optical communication applications, low photosensitivity characteristics are advantageous in control units used for electronic switching devices [3, 16-18]. It was observed that the photosensitivity of the photodiodes can be effectively tuned by varying the B_4C doping ratio, and the fabricated devices exhibited clear photoconductive behavior.

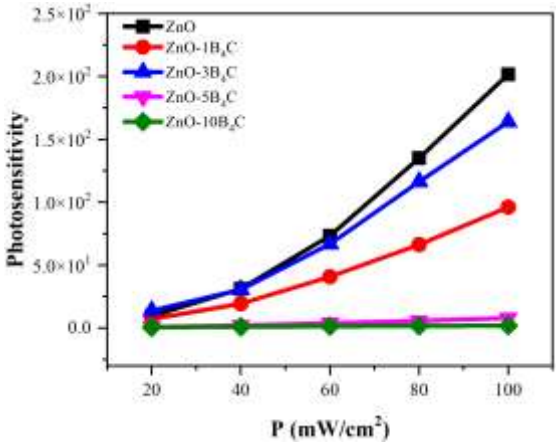

Figure 3. Photosensitivity of the photodiodes under different light intensities.

The time-dependent photocurrent characterization of photodiodes plays a crucial role in understanding their photoconductive mechanisms and charge transport behavior. The transient photocurrent responses of the fabricated photodiodes measured at -3 V under different illumination intensities between 20 and 100 mW/cm^2 are presented in Figure 4. With increasing light intensity a noticeable rise in photocurrent was observed, which can be attributed to the generation of a higher number of charge carriers within the depletion region. The steady increase in photocurrent with illumination demonstrates that the fabricated devices exhibit strong and stable photoconductive behavior, indicating their effective response to incident light [3, 18, 19]. Under illumination, the formation and increase in the number of free charge carriers caused the photocurrent to reach a saturation level, while photogenerated electrons further contributed to the overall current. When the illumination was turned off, the photocurrent rapidly returned to its initial level due to the release and recombination of charge carriers trapped at deep energy states. This repetitive rise and decay behavior upon successive light on and off cycles revealed that the fabricated photodiodes possess reversible and stable switching characteristics [3, 20, 21]. At a light intensity of 100 mW/cm^2, the photocurrent values of the ZnO photodiodes containing 0%, 1%, 3%, 5%, and 10% B_4C were determined as 56×10^{-4} A, 16.4×10^{-5} A, 6.97×10^{-5} A, 3.43×10^{-5} A, and 2.67×10^{-5} A, respectively. It was observed that the photocurrent decreased with the addition of B_4C and continued to decline as the doping concentration increased. This reduction in photocurrent can be attributed to the higher B_4C content, which is believed to increase the carrier concentration within the ZnO matrix. The elevated carrier density may distort the surface electric field, thereby reducing carrier mobility and resulting in longer photoresponse times [3, 22, 23]. The photoresponse characteristics of the photodiodes can be effectively controlled and tuned by varying the B_4C doping ratio.

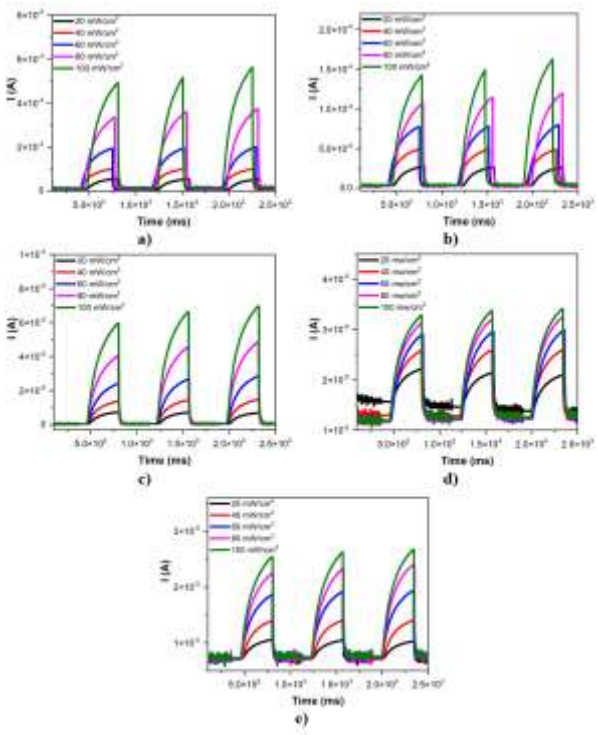

Figure 4. I-t graphs of a) ZnO, b) ZnO:1%B_4C, c) ZnO:3%B_4C, d) ZnO:5%B_4C and e) ZnO:10%B_4C devices.

4. Conclusion

Based on the comprehensive structural, electrical, and photoresponse analyses, the following conclusions were drawn regarding the performance and behavior of the fabricated Al/p-Si/ZnO:B_4C /Al photodiodes:

- Al/p-Si/ZnO:B_4C/Al photodiodes were successfully fabricated using the sol-gel spin coating technique, producing uniform, crack-free, and nanostructured thin films on p-Si substrates.
- FE-SEM and EDX analyses confirmed the homogeneous distribution of Zn, O, B, and C elements in the films and verified the successful

incorporation of B_4C into the ZnO matrix without secondary phase formation.

- Increasing the B_4C content led to a reduction in grain size and improved surface uniformity, indicating that B_4C enhances the structural and morphological properties of ZnO thin films.
- All fabricated photodiodes exhibited strong sensitivity to light and clear photoconductive behavior under illumination, confirming their effective photoresponse.
- The photocurrent values measured at 100 mW cm^{-2} illumination were 56 x 10^{-4}, 16.4 x 10^{-5}, 6.97 × 10^{-5}, 3.43 x 10^{-5}, and 2.67 x 10^{-5} A for 0%, 1%, 3%, 5%, and 10% B_4C doping levels, respectively.
- The photocurrent decreased as the B_4C concentration increased, which was attributed to changes in carrier density and mobility caused by the dopant.
- The photoresponse characteristics could be tuned by adjusting the B_4C doping ratio, demonstrating controllable and stable device behavior.
- Transient photocurrent measurements showed fast, reversible, and repeatable responses under light on/off cycles, confirming the switching stability of the photodiodes.
- The results revealed that optimal B_4C doping can enhance interface quality and electrical stability, while excessive doping reduces photoresponse efficiency.
- Overall, ZnO:B_4C composite photodiodes exhibit promising potential for optoelectronic and photodetection applications due to their controllable, stable, and reproducible photoelectric performance.

Acknowledgment

This research was supported by the Scientific Research Projects Coordination Unit of Fırat University (FÜBAP) under project number TEKF.23.43. The study was conducted by Mahmud ALLAVI and is derived from his master's thesis entitled "Fabrication of Al/p-Si/ZnO:B_4C/Al Photodiodes by Sol-Gel Spin-Coating Method and Determination of Their Photoresponse and Electrical Properties."

References

[1] Aslan, F., H. Esen, F. Yakuphanoglu, Optik 197 (2019) 163203.
[2] N. Khusayfan, J. Mol. Struct. 1224 (2021) 129030.
[3] E. Gürgenç, A. Dikici, F. Aslan, Physica B: Condensed Matter. 639 (2022) 413981.
[4] Y.I. Alivov, J. Van Nostrand, D.C. Look, M. Chukichev, B. Ataev, Appl. Phys. Lett. 83 (2003) 2943-2945.
[5] A. Karaca, D.E. Yıldız, M. Yıldırım, Phys. Scr. 99 (2024) 115904.
[6] M. Karyaoui, Silicon (2025) 1-10, Doi: 10.1007/s12633-025-03475-5.
[7] A. Tursucu, S. Aydogan, A. Kocyigit, A. Ozmen, M. Yilmaz, JOM 74 (2022) 777-786.
[8] C. Ozel, C.K. Macit, T. Gurgenc, F. Biryan, E. Gurgenc, S. Bellucci, Appl. Phys. A 130 (2024) 232.
[9] C.K. Macit, E. Gurgenc, F. Biryan, F. Özen, T. Gurgenc, C. Ozel, J. Mater. Sci. Mater. Electron. 34 (2023) 2076.
[10] A. Tataroğlu, A.A. Al-Ghamdi, S.B. Omran, W. Farooq, F. El-Tantawy, F. Yakuphanoglu, J. Sol-Gel Sci. Technol. 71 (2014) 421-427.
[11] M. Caglar, K. Sever, S. Aktas, A. Demiroglu, Sens. Actuators A Phys. 350 (2023) 114099.
[12] A. Tataroğlu, A. Hendi, R. Alorainy, F. Yakuphanŏlu, Chin. Phys. B 23 (2014) 057504.
[13] Y. Liu, Y. Li, H. Zeng, J. Nanomater. 2013 (2013) 196521.
[14] E.I. Ugwu, Sol-Gel Method - Design Synth. New Mater. Phys. Chem. Biol. Prop. (2018).
[15] H.A. Thabit, N.A. Kabir, A.K. Ismail, S. Alraddadi, A. Bafaqeer, M.A. Saleh, Nanomaterials 12 (2022) 3068.
[16] S. Dugan, M.M. Koç, B. Coşkun, J. Mol. Struct. 1202 (2020) 127235.
[17] S.A. Pehlivanoglu, Phys. B Condens. Matter 603 (2021) 412482.
[18] F. Aslan, H. Esen, F. Yakuphanoglu, J. Alloys Compd. 789 (2019) 595-606.
[19] N.A. Elkanzi, A. Farag, N. Roushdy, A. Mansour, Optik 216 (2020) 164882.
[20] R. Gupta, A. Hendi, M. Cavas, A.A. Al-Ghamdi, O.A. Al-Hartomy, R. Aloraini, F. El-Tantawy, F. Yakuphanoglu, Phys. E Low-Dimens. Syst. Nanostruct. 56 (2014) 288-295.
[21] M. Rajini, S. Vinoth, K. Hariprasad, M. Karunakaran, K. Kasirajan, N. Chidhambaram, T. Ahamad, S.M. Alshehri, Appl. Phys. B 127 (2021) 1-11.
[22] K. Thiyagarajan, B. Saravanakumar, S.-J. Kim, ACS Appl. Mater. Interfaces 7 (2015) 2171-2177.
[23] X. Zhang, Z. Shao, X. Zhang, Y. He, J. Jie, Adv. Mater. 28 (2016) 10409-10442.